Effect of interface viscosity on the breakup of liquid sheets

Vitor H. C. Cunha, Sergio S. Ribeiro, Marcio S. Carvalho

Dept. of Mechanical Engineering, Pontifical Catholic University of Rio de Janeiro
R. Marquês de São Vicente 225, 22541-041, Rio de Janeiro, Brazil
heitorvitorc@gmail.com; sergio@lmmp.mec.puc-rio.br; msc@puc-rio.br

Abstract. Free surface flow is of major relevance in many fluid dynamics applications, both at the macroscopic scale, like in the study of water waves and the design of watercraft, and at the microscopic scale, such as in thin films and microfluidics. Understanding the physical mechanisms contributing to the stability of thin liquid sheets is a challenging problem, as they present a fluid-fluid interface which is free to deform. In systems with high surface area to volume ratios, such as micro bubbles, blood cells and emulsions, the dynamics of the system are also highly influenced by the dynamics on the interface. In addition, the presence of surface-active agents such as polymers and surfactants may lead to complex interfacial rheological behavior. In this work, a computational investigation of the breakup dynamics of a stationary thin liquid sheet bounded by a passive gas with a viscous interface is presented. An Arbitrary Lagrangian-Eulerian method (ALE) is used to track the interface position. The rheological behavior of the interface is modeled by the Boussinesq-Scriven law, and the numerical solution is obtained through finite element approximation. The results show that the stability of free surfaces is influenced by surface rheology and that the viscous character of the interface delays the sheet breakup, leading to more stable films.

Keywords: surface flow; viscous interfaces; interfacial rheology; Boussinesq-Scriven; free thin liquid films

1 Introduction

1.1 Motivation

Free surface flows have fascinated scientists and practitioners over many decades with several theoretical and experimental challenges and can generate a host of alluring behaviors due to its movement. The flow of a free thin liquid sheet is an intrinsic example of a free surface flow, as its surfaces typically have their own dynamic properties from which surface tension effects and complex interfacial rheological behavior arises. In nature, the rupture of thin liquid films bounded by a solid substrate and a free surface is one of the core mechanisms in common health conditions, such as the dry eye syndrome and the respiratory distress syndrome (Zhong et al. [1]; Jensen and Grotberg [2]). Industrial applications such as aerosol droplet generation (Collins et al. [3]), inkjet printing (Chung et al. [4]) and monodisperse emulsions fabrication (Shah et al. [5]) rely on the rupture of thin liquid sheets in their procedure. However, the breakup process of thin films can be undesirable in applications such as slot die and spin coating (Sampaio et al. [6]), in which the additional layer may perform specific roles, such as electric conduction, heat isolation and protection.

Liquid–liquid and liquid-gas surface forces play a key role in the stability of thin liquid sheets. Depending

on the problem scale different behavior must be considered, that may oppose or yield interfacial tension between the phases. In most practical applications, the instability of a thin liquid sheet is driven by long-range molecular forces due to van der Waals attractions, whereas capillary and viscous forces have a stabilizing effect (Erneux and Davis [7]; Bazzi and Carvalho [8]). The liquid film rupture occurs when it is sufficiently thin, in which the long-range intermolecular forces become dominant (Craster and Matar [9]). Considering the rupture dynamics, the ultimate lifetime of liquid films is determined by two processes: thinning and growth of surface fluctuations, and the rupture gives rise to a finite time singularity in the governing equations. In both nature and industry, these surface fluctuations are often stabilized by the presence of surface-active agents such as surfactants that can extend the life span of thin films in a considerable manner by reducing the drainage rate of the thin films during the rupture evolution.

1.2 Objectives

The study of free thin liquid film dynamics may give insights that can lead to many technological breakthroughs in areas such as photovoltaic systems, thin sheet solid state batteries, lithography, additive manufacturing and ultrathin polymeric coating. The underlying rupture mechanisms of these flows are encompassed in a complex interplay between capillarity, hydrodynamics and interfacial stresses and are of utmost importance for quality control, reliability and reproducibility of industrial processes. In this paper, we will study the influence of interface rheology on the dynamics of stationary free surface thin liquid films concerning a continuum approach, as assumed to be valid for water-like bulks of ~1-2 nm thickness (Bocquet and Charlaix [10]). We aim at understanding the mechanisms by which surface stresses caused by interfacial viscosity delay the breakup time of a stationary free thin liquid sheet.

2 Literature review

The instability of free liquid sheets is strongly influenced by the interplay between capillary pressure, long range intermolecular van der Waals attractions and hydrodynamic pressure, which was first analyzed by Taylor [11], aiming to understand the wave propagation on the surface of free films. In his work, he identified that the surface of the free liquid sheet can exhibit two distinct dynamical modes: an antisymmetric or stretching mode where the free liquid film buckles; and a symmetric or squeezing mode, in which the opposite surfaces move towards each other, urging the possibility of film rupture. The understanding of thin film rupture was extended theoretically by the derivation of a nonlinear evolution equation for the thickness of a thin film on a solid substrate by Williams and Davis [12]. In their study, a nonlinear partial differential equation is solved by numerical methods, which resulted in a characteristic rupture time calculation 10 times smaller than rupture time obtained from previous linear approaches. Erneux and Davis [7] used the long wavelength approximation along with the Navier-Stokes equations with an extra term to encompass the van der Waals attraction to derive asymptotically a system of governing nonlinear evolution equations for longitudinal velocity and film thickness. Ida and Miksis [13] then solved numerically the set of equations proposed by Erneux and Davis [7] and examined the dominant balances in the evolution equations using similarity-times solutions in the temporal and spatial vicinity of rupture.

The influence of the chemical composition of a free surface has long been recognized to change its dynamics, as complex fluid interfaces are often characterized by the presence of amphiphilic molecules such as surface-active agent (surfactants), proteins and particles that induces microstructures with significant mechanical strength, along with possible thermodynamic complexities (Scriven [14]). Interfacial rheology describes the functional relationship between the deformation of such complex interface, the stresses exerted in and on it and the resulting flows in the adjacent fluid phases (Leopércio [15]). Jensen and Grotberg [2] used lubrication theory to study the spreading rate of a localized monolayer of insoluble surfactant on the surface of a thin viscous film, in the limit of weak capillary and weak surface diffusion, and stated that the presence of insoluble surfactants decreases the growth rate of the instability, but do not affect critical wavelengths, and the stabilizing influence of surfactants remains relatively weak. Vaynblat et al [16] extended the studies on the rupture dynamics by introducing two main rupture geometries, line rupture and point rupture for free viscous films exhibiting both simple Newtonian and more complex power-law rheology, and analyzed the self-similar dynamics that arise during sheet rupture. Becerra and Carvalho [17] proceeded with an examination regarding the flow of free viscoelastic liquid sheets occurring

in curtain coating processes and showed that high extensional viscosity due to rheological behavior of polymer solutions on the flow create more stable curtains. Bazzi and Carvalho [8] also addressed the effect of viscoelastic properties of polymer solutions of the breakup process of a free liquid sheet by extending the stability criterion proposed by Erneux and Davis [7] for axisymmetric perturbations and Oldroyd-B liquids, and showed through numerical solutions that the effect of rheology slows down the perturbation growth drastically and thus slowing the sheet rupture.

Moreover, the flow of free thin liquid sheets is an intrinsic example of multiphase flow, and the temporal evolution of fluid phases in a multiphase flow is often a very difficult task to predict due to their dependence on several parameters such as geometry, fluid properties and flow regime, and are commonly characterized in dispersed flows and separated flows (Kassar [18]). Numerical simulations of multiphase flows rely mainly on a Multi-Fluid model and a One-Fluid model approaches, in which one may consider two basic viewpoints in discretizing a fluid region by a finite element method, namely Lagrangian and Eulerian reference systems (Prosperetti and Tryggvason [19]). In a Lagrangian system, the mesh of grid points is embedded in the fluid and moves with it with correspondent velocity $\boldsymbol{v}$, while a Eulerian reference system treats the computational mesh as a fixed reference frame through which the fluid motion is described in terms of spatial coordinates. The Front-Tracking method (Unverdi and Tryggvason [20]) and the Marker and Cell (MAC) method (Harlow and Welch [21]; Daly [22]) are examples of tracking strategies employed through a Lagrangian reference system and track and follow the interface according to the local velocity explicitly and implicitly, respectively; whereas the Volume of Fluid (VOF) method (Prosperetti and Tryggvason [19]) and the Level-Set (LS) method (Osher and Sethian [23]) are popular examples of Eulerian interface tracking methods.

Furthermore, the shortcomings of purely Lagrangian and Eulerian descriptions lead to the development of an alternative technique that combines the best features of both descriptions in a mixed manner, known as the Arbitrary Lagrangian-Eulerian (ALE) description. The ALE description represents a generalization of the two previous methods and treats the computational mesh as a reference frame which may be moving with an arbitrary velocity $\boldsymbol{\omega}$ (Hughes et al. [24]). If $\boldsymbol{\omega} = 0$, the reference frame is fixed in space and corresponds to the Eulerian coordinate system, whereas $\boldsymbol{\omega} = \boldsymbol{v}$ indicates that the reference frame moves in space at the same velocity as the grid points, corresponding to the Lagrangian reference system. For the case $\boldsymbol{\omega} \neq \boldsymbol{v} \neq 0$, the reference system is called arbitrary Lagrangian-Eulerian frame and moves in space at a velocity $\boldsymbol{\omega}$.

3 Methodology

In this work we consider the One-Fluid model to numerically analyze the breakup dynamics of a 2D stationary free thin liquid sheet, considering the effects of surface tension, surface viscosity and van der Waals forces and under a symmetric perturbation regarding Taylor's dynamical modes. A symmetry plane on the x axis is taken into account to ease the computational cost of the simulation. We consider that the surrounding gaseous phase is inert and therefore does not interact with the thin liquid sheet, and the system is considered incompressible and isothermal. The bulk hydrodynamics will be taken through the continuum approach, by means of the continuity equation for the conservation of mass and the Navier-Stokes equations for the conservation of linear momentum. The absence of mass transfer across the interface places a kinematic restriction on the normal velocity of the interface, and assuming that there is no slip between the phases means that the tangential velocity of each phase is equal and that there are no constraints in the tangential direction of the fluid velocity at the interface. A general expression for the interfacial stress σ_s for a complex interface is given by Slattery et al. [25] as,

$$\sigma_s = \sigma(\Gamma_c, T)I_s + \sigma_e \tag{1}$$

in which $\sigma(\Gamma_c, T)$ is the surface tension which depends on the excess concentration Γ_c and temperature T, I_s is the surface unit tensor that transforms every vector into its component tangential to the interface and σ_e is the surface extra stress. The interfacial tension term $\sigma(\Gamma_c, T)$ encompasses the convection of surfactants with the surface flow, which may yield non-uniform distribution on the interface and result in non-constant interfacial tension. Marangoni advection and gravity effects are neglected in our study, hence the term $\sigma(\Gamma_c, T)I_s$ reduces to the Young-Laplace law for interfacial stress, resulting in

$$\sigma_s = \sigma_{\alpha\beta}I_s + \sigma_e \tag{2}$$

A general form of equations for a linear dependence of stress on rate of strain in the interface was first

introduced by Boussinesq [26] and later generalized by Scriven [14] to account for the evolution of Newtonian fluids in the interfacial state. Hence, for a liquid-like viscous interface, the extra stress can be described by the Boussinesq-Scriven model

$$\sigma_e = (\kappa_s - \mu_s)(\nabla_s \cdot \vec{u})I_s + 2\mu_s D_s \tag{3}$$

where κ_s is the interfacial dilatational viscosity, μ_s interfacial shear viscosity, $\nabla_s = I_s \cdot \nabla$ is the surface gradient operator, $\vec{u}_s$ is the free surface velocity vector and $D_s = 1/2\,[\nabla_s \vec{u}_s \cdot I_s + I_s \cdot (\nabla_s \vec{u}_s)^T]$ is the surface rate-of-deformation tensor. Therefore, the surface stress is resumed by the following equation

$$\sigma_s = \sigma_{\alpha\beta} I_s + (\kappa_s - \mu_s)(\nabla_s \cdot \vec{u})I_s + 2\mu_s D_s \tag{4}$$

The free surface is thought of as a sharp interface and the extra stress term of the viscous interface is modeled by the Boussinesq-Scriven constitutive law. The system is implemented through the Finite Element Method, namely using the Galerkin method and triangular finite elements in an unstructured mesh. The free surface is tracked through the Arbitrary Lagrangian-Eulerian method. The numerical methods are implemented in Python through the FEniCs open-source library.

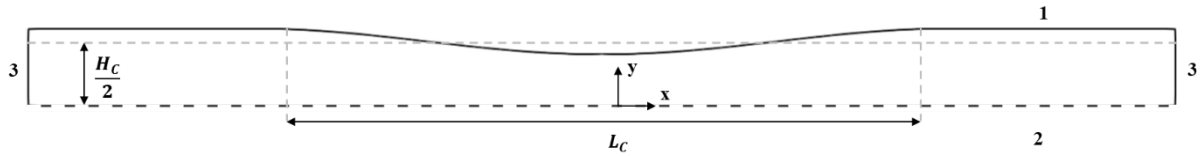

Figure 1. Initial configuration of the stationary free thin liquid sheet

Figure 1 represents the initial configuration of the domain, in which H_C is the undisturbed film thickness, L_C is the perturbation wavelength and $\Gamma = 1 \cup 3 \cup 2 \cup 3$ is the domain boundary. Therefore, the boundaries are defined as: top boundary (**1**) is a free moving surface; bottom boundary (**2**) is considered a symmetry plane; left and right boundaries (**3**) are considered free to flow along with a negligible pressure gradient across the thin film cross section. The interface position is denoted as $h(x,t) \in 1$, the initial conditions used are $u(x,y,t=0) = 0$ and $h(x,t=0) = H_C/2 - \epsilon \cos(\pi x)$, where ϵ is the perturbation amplitude. The region of minimum thickness is located at $x = 0$ and the simulation ends when $h(x=0,t) \leq 0.1H_C$. According to Erneux and Davis [7] in the limit of $H_C/L_C \ll 1$, the free thin liquid sheet is stable when

$$\frac{S}{A} \geq \frac{2}{\pi^2} \tag{5}$$

where $S = \sigma_{\alpha\beta}\,\rho H_C/3\mu^2$ is a nondimensional constant that accounts the dimensional surface tension $\sigma_{\alpha\beta}$ and $A = \rho L_C\,\tilde{A}/6\pi H_C^3\mu^2$ is a dimensionless constant which encompasses the van der Waals effects through the Hamaker constant $\tilde{A}$.

3.1 Governing equations

Considering the One-Fluid model, the conservation of mass, in the absence of mass transfer, is given by

$$\nabla \cdot \vec{u} = 0 \tag{6}$$

The conservation of linear momentum is given by the Navier-Stokes equations

$$\rho\left(\frac{\partial \vec{u}}{\partial t} + \vec{u} \cdot \nabla\vec{u}\right) = \nabla \cdot T \tag{7}$$

in which $T(\vec{u}, p) = -pI + 2\mu\epsilon(\vec{u})$ is the Cauchy stress tensor and $\epsilon(\vec{u}) = [\nabla\vec{u} + (\nabla\vec{u})^T]$ is the rate-of-deformation tensor. The parameters ρ and μ are the bulk density and absolute viscosity, respectively. To ensure that a unique solution of the system exists, the following boundary conditions are implemented according to the respective boundary:

$$\text{symmetry (2)} \;\rightarrow\; = \frac{\partial u_x}{\partial y} = 0\,,\, u_y = 0 \tag{8}$$

$$\text{left and right } (\mathbf{3}) \;\rightarrow\; \frac{\partial \vec{u}}{\partial x} = 0 \tag{9}$$

Also, we consider a zero pressure gradient in the y direction of left and right boundaries, which means that the pressure along the left and right boundaries are equal to the pressure at the point of intersection between left/right boundary and the free surface $y_{L/R}$. Since the surface stress acts on the tangential direction of the interface, the boundary condition is taken as the normal-direction van der Waals force acting on the surface point of each lateral boundary respectively. The additional boundary condition is implemented as follows

$$\text{left and right } (\mathbf{3}) \;\rightarrow\; p = \tilde{A}/2\pi y_{L/R} \tag{10}$$

Furthermore, the motion of the interface is coupled with the bulk velocity according to

$$\text{free surface } (\mathbf{1}) \;\rightarrow\; \hat{n} \cdot \vec{u} = \hat{n} \cdot \frac{dx}{dt} \tag{11}$$

The jump of traction across the interface is taken in two cases, namely a simple or inviscid interface with no extra stresses and a viscous interface with an extra stress modeled by the Boussinesq-Scriven law. The stress balance across the free surface (**1**) is imposed by the following equation

$$\text{free surface } (\mathbf{1}) \;\rightarrow\; \hat{n} \cdot T = \nabla_s \cdot \sigma_s - (p_s + \Phi) I_s \tag{12}$$

where the sum of the surface pressure p_s with the long-range intermolecular van der Waals potential $\Phi = \tilde{A}/2\pi y^3$ is taken as a disjoining pressure while the interface stress tensor σ_s is depicted by Eq. 4.

4 Results and discussion

The system configuration will take into account parameters that break the stability criterion presented in Eq. 5, namely for the ratio $S/A = 1/\pi^2$. The domain is configured for $H_C = 10\mu m$ and $L_C = 10H_C$, with a symmetric perturbation $\epsilon = 0.1H_C$. Also, we introduce the dimensionless numbers for the analysis of the problem: capillary number $Ca = \mu\, u/\sigma_{\alpha\beta}$ and Boussinesq number $Bo = \eta_s/\mu H_C$ with $\eta_s = \kappa_s + \mu_s$ as a "total" interfacial viscosity. The results presented in this section are obtained for $Ca = 2$ and $Bo \in [0,1]$. When $Bo = 0$, interfacial viscosity effects are off the surface dynamics, which yields the simple surface case. Analogously, the effects of interfacial rheology become prominent as Bo increases. Figure 2 depicts snapshots of the pressure field for $Bo = 0$ in $t = 0$ and $t_r = 4.3 \times 10^{-4}$s, ordered from top to bottom, respectively. The effects of long-range van der Waals forces act on the region of minimum thickness, which yields a pressure gradient that drives the drainage of the film. The results obtained are in accordance with the stability criterion presented in Eq. 5.

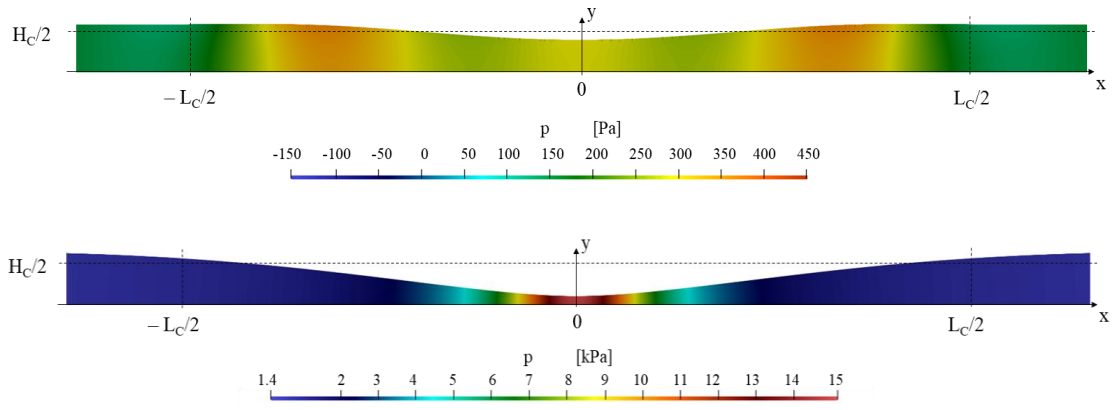

Figure 2. Pressure field snapshots from $t_i = 0$ s (top) and $t_r = 4.3 \times 10^{-4}$s (bottom).

The capillary pressure caused by the surface curvature opposes the disjoining pressure, resulting in a local pressure gradient towards $x = 0$, as illustrated by Figure 2 (top). However, the occurrence of curvature diffusion due to the sheet drainage reduces the influence of capillarity on the delay of the rupture process. Figure 3 (left) presents the evolution of the region of minimum thickness towards the thin liquid film rupture. The nonlinear

profile of the thin film thickness is associated with the increase of long-range intermolecular attractions as the thin film thins.

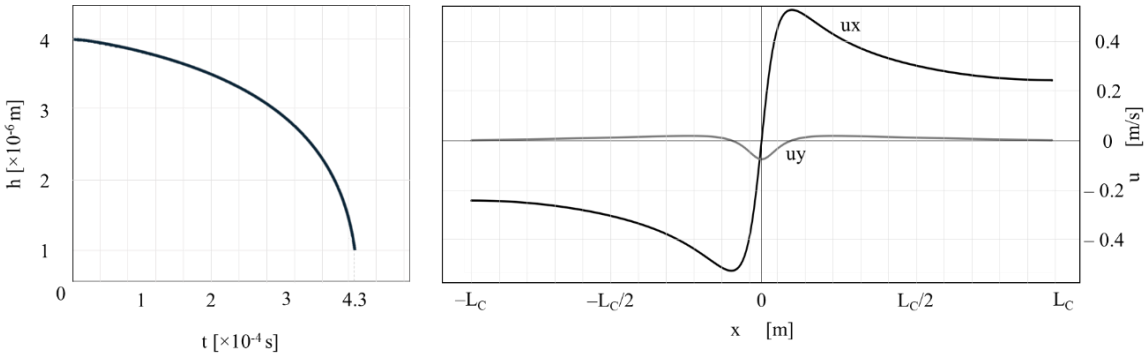

Figure 3. Evolution of the free surface thickness $h(x = 0, t)$ (left) and x and y components of the velocity vector at the free surface at $t_r = 4.3 \times 10^{-4}$s (right).

Figure 3 (right) presents the x and y components of the velocity field at the surface at rupture time $t_r = 4.3 \times 10^{-4}$s. The drainage rate is driven by the velocity x component, which increases as van der Waals effects become dominant over the free surface movement at $x = 0$, leading the system into a finite time singularity. The presence of an interfacial viscosity affects the surface mobility, as an extra surface stress opposes the disjoining pressure. Figure 4 (left) shows the time evolution of the thin film thickness h at $x = 0$ for $Bo \in [0,1]$. The additional forces from interfacial viscosity increase the rupture time of the thin liquid film, as presented in Figure 4 (right). Moreover, the effects of interfacial rheology obtained from our simulations did not change the results predicted by the stability criterion.

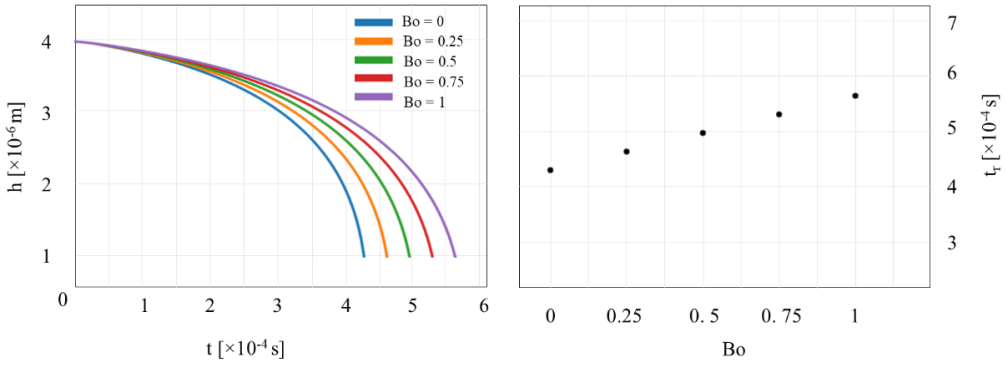

Figure 4. Evolution of the free surface thickness $h(x = 0, t)$ (left) for $Bo \in [0,1]$ and rupture time t_r as function of the Boussinesq number Bo (right).

Figure 5 illustrates the velocity of the interface at each rupture time presented in Figure 4 (right). As Bo increases, the surface velocity reduces both in the x and y components, as respectively shown in Figure 5 (top) and (bottom). The reduction in the surface velocity yields in a reduction of surface mobility, which may be accounted for the rupture delay as Bo increases.

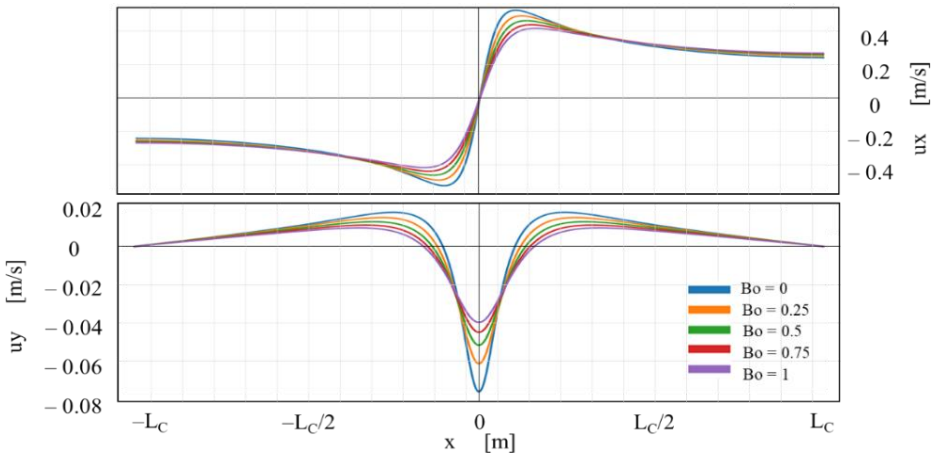

Figure 5. Evolution of the free surface thickness $h(x = 0, t)$ (left) for $Bo \in [0,1]$ and x and y components of the velocity vector at the free surface at $t_r = 4.3 \times 10^{-4}$s (right).

5 Conclusion

We addressed the response of a stationary Newtonian thin liquid sheet to a symmetric perturbation under the influence of capillarity and surface viscous effects that resist the long-range intermolecular attraction between each free surface of the liquid sheet. The effect of surface viscous forces on the rupture process of a free thin liquid was analyzed by solving the governing equations presented in section 3. For an initial perturbation of $\epsilon = 0.2H_C$, the system follows the behavior predicted by the weakly linear stability criterion proposed by Erneux and Davis (1995). The numerical solution of the governing equations revealed that the presence of interface viscosity increases the rupture time, as shown in Figure 4 (right). The effects of the rheological behavior of the interface also reduced its mobility as a result of the additional stresses presented on the system dynamics. The results also show that viscous forces have a considerable effect on the dynamics of the sheet rupture, albeit not having any effect on the value of S/A.

Acknowledgements. This work was partially funded by CAPES, Financial code 0001.

Authorship statement. The authors hereby confirm that they are the sole liable persons responsible for the authorship of this work, and that all material that has been herein included as part of the present paper is either the property (and authorship) of the authors, or has the permission of the owners to be included here.

References

[1] L. Zhong, C. Ketelaar and R. Braun. Mathematical modelling of glob-driven tear film breakup. Mathematical Medicine and Biology, Vol. 26, pp.55-91, 2019.
[2] O. Jensen and J.B. Grotberg. Insoluble surfactant spreading on a thin viscous film: shock evolution and film rupture. Journal of Fluid Mechanics, Vol. 240, pp. 259-288,1992.
[3] D. Collins, O. Manor, A. Winkler, H. Schmidt, J.R. Friend and L.Y. Yeo. Atomization of thin water films generated by high-frequency substrate wave vibrations. Physical Review, Vol. 86, 2012.
[4] S. Chung, K. Cho and T. Lee. Recent progress in inkjet-printed thin-film transistors. Advanced Science, Vol. 6, 2019.
[5] R.K. Shah, H.C. Shum, A.C. Rowat, D. Lee, J.J. Agresti, A.S. Utada, L.Y. Chu, J.W. Kim, A. Fernandez-Nieves, C.J. Martinez and D.A. Weitz. Designer emulsions using microfluidics. Materials Today, Vol. 11, No. 4, pp. 18-27, 2008.
[6] P.G.V. Sampaio, M.O.A. González, P.O. Ferreira, P.C.J. Vidal, J.P.P. Pereira, H.R. Ferreira and P.C. Oprime. Overview of printing and coating techniques in the production of organic photovoltaic cells. Int. J. Energy Research, Vol. 44, pp. 9912-9931, 2020.
[7] T. Erneux and S.H. Davis. Nonlinear rupture of free films. Physics of Fluids A, Vol. 5, pp. 1117-1122, 1993.
[8] M.S. Bazzi and M.S. Carvalho. Effect of viscoelasticity on liquid sheet rupture. Journal of Non-Newtonian Fluid Mechanics, Vol. 264, pp. 107-116, 2019.

[9] R. Craster and O. Matar. Dynamics and stability of thin liquid films. Reviews of Modern Physics, Vol. 81, pp.1131-1198, 2009.
[10] L. Bocquet and E. Charlaix. Nanofluidics, from bulk to interfaces. Chem. Soc. Rev., Vol. 39, pp. 1095, 2010.
[11] G. Taylor. The dynamics of thin sheets of fluid II: waves on fluid sheets. Proceedings of the Royal Society of London A, Vol. 253, pp. 296-312, 1959.
[12] M.B. Williams and S.H. Davis. Nonlinear theory of film rupture. Journal of Colloid and Interface Science, Vol. 90, No. 1, pp. 220-228, 1982.
[13] M.P. Ida and M.J. Miksis. Thin film rupture. Applied Mathematics Letters, Vol. 9, pp. 35-40, 1995.
[14] L.E. Scriven. Dynamics of a fluid interface. Chemical Engineering Science, Vol. 12, pp. 98-109, 1960.
[15] B. C. Leopércio. Kinetics of cyclopentane hydrate formation – an interfacial rheology study. MSc dissertation, Pontifical Catholic University of Rio de Janeiro, 2016.
[16] D. Vaynblat, J.R. Lister and T.P. Witelski. Rupture of thin viscous films by van der Waals forces: evolution and self-similarity. Physics of Fluids, Vol. 13, No. 5, 2001.
[17] M. Becerra and M.S. Carvalho. Stability of viscoelastic liquid curtain. Chemical Engineering and Processing: Process Intensification, Vol. 50, pp. 445-449, 2011.
[18] B.B.M. Kassar. Numerical simulation of multiphase flows with enhanced curvature computation by point-cloud sampling. PhD thesis, Pontifical Catholic University of Rio de Janeiro, 2016.
[19] A. Prosperetti and G. Tryggvason. *Computational methods for multiphase flow*. Cambridge University Press, 2007.
[20] S.O. Unverdi and G. Tryggvason. A front-tracking method for viscous, incompressible, multi-fluid flows. Journal of Computational Physics, Vol. 100, pp. 25-37, 1992.
[21] F.H. Harlow and J.E. Welch. Numerical calculation of time-dependent viscous incompressible flow of fluid with free surface. Physics of Fluids, Vol.8, pp. 2182-2189, 1965.
[22] B.J. Daly. Numerical study of two-fluid Rayleigh-Taylor instability. Physics of Fluids, Vol. 10, pp. 297-307, 1967.
[23] S. Osher and J.A. Sethian. Fronts propagating with curvature-dependent speed: Algorithms based on Hamilton-Jacobi formulations. Journal of Computational Physics, Vol. 79, pp. 12-49, 1988.
[24] T.J.R. Hughes, W.K. Liu and T.K. Zimmermann. Lagrangian-Eulerian Finite Element formulation for incompressible viscous flows. Computer Methods in Applied Mechanics and Engineering, Vol. 29, pp. 329-349, 1981.
[25] J.C. Slattery, L. Sagis and E.S. Oh. Interfacial transport phenomena. Springer Science & Business Media, 2007.
[26] J. Boussinesq. Existence of a superficial viscosity in the thin transition layer separating one liquid from another contiguous fluid. C. R. Acad. Sci., Vol. 156, pp. 983–89, 1913.